Research Article

Fe/Indonesian Natural Zeolite as Hydrodeoxygenation Catalyst in Green Diesel Production from Palm Oil

Riandy Putra[1], Witri Wahyu Lestari[2*], Fajar Rakhman Wibowo[1], Bambang Heru Susanto[3]

[1]*Master of Chemistry Program, Graduate School, Sebelas Maret University, Jl. Ir. Sutami No.36A, Kentingan, Jebres, Surakarta, 57126, Indonesia*
[2]*Research Group of Porous Material for Sustainability, Chemistry Department, Faculty of Mathematics and Natural Sciences, Sebelas Maret University, Jl. Ir. Sutami No.36A, Kentingan, Jebres, Surakarta, Central Java, 57126, Indonesia*
[3]*Department of Chemical Engineering, Faculty of Engineering, Universitas Indonesia, Kampus UI Depok, Depok, 16424, Indonesia*

Abstract

The Petroleum diesel-based fossil fuel remains the primary source of energy consumption in Indonesia. The utilization of this unrenewable fuel depletes fossil fuels; thus, an alternative, renewable fuel, such as one based on bio-hydrocarbon from biomass-green diesel-could be an option. In this work, green diesel was produced through the hydrodeoxygenation from palm oil and processed in a batch-stirred autoclave reactor over natural zeolite (NZ) and NZ modified with 3 wt.% Fe metal (Fe/NZ) as heterogeneous catalyst. NZ showed high crystallinity and suitability to the simulated pattern of the mordenite and clinoptilolite phases according to X-ray diffraction (XRD) analysis. The presence of Fe metal was further confirmed by XRD, with an additional small diffraction peak of Fe^0 that appeared at $2\theta = 44\text{-}45°$. Meanwhile, NZ and Fe/NZ were also characterized by Scanning electron microscopy (SEM) with Energy Dispersive X-ray (EDX), X-ray Fluorescence (XRF), and Surface Area Analyzer (SAA). The obtained materials were tested for the conversion of palm oil into diesel-range hydrocarbons (C_{15}-C_{18}) under conditions of 375 °C and 12 bar H_2 for 2 h. NZ and Fe/NZ produced a liquid hydrocarbon with straight-chain (C_{15}-C_{18}) alkanes as the most abundant products. Based on Gas Chromatography-Mass Spectrometry (GC-MS) measurement, a higher conversion of palm oil into diesel-like hydrocarbons reached more than 58% and 89%, when NZ and Fe modified NZ (Fe/NZ), respectively were used as catalysts. Copyright © 2018 BCREC Group. All rights reserved

Keywords: Indonesian Natural Zeolite; Iron Metal; Hydrodeoxygenation; Palm Oil; Green Diesel

1. Introduction

The production of renewable feedstocks-based fuels from vegetable oil has been recent interest to solve the problems of the depletion of crude oil reserves, shortages in petroleum supply, and the utilization of nonrenewable fuel in some sectors. Biodiesel could be a promising option to be used for diesel-based oil engine transportation. The drawbacks of biodiesel has high viscosity, low oxidative stability, a high cloud point, nitrogen oxide (NO_x) emissions, injector/engine wear, and low energy density [1]. Hydrodeoxygenation (HDO) of vegetable oil has been investigated as an alternative pathway for biofuel production to avoid these physical and

* Corresponding Author.
   E-mail: witri@mipa.uns.ac.id (W.W. Lestari)
   Telp: +62-82-227833424, Fax: +62-27-1663375

chemical shortcomings. Among the vegetable oils, palm oil has great potential due to its abundant production in Indonesia and high levels of palmitic acid and oleic acid content [2]. HDO is a type of hydrotreating reaction in which oxygen is removed from an oxygen-containing compound under high-pressure hydrogen conditions at high temperature with the help of a metal as a heterogeneous catalyst; the resulting product is known as green diesel [3]. This type of biofuel possesses hydrocarbon *n*-paraffin (C_xH_y) structures containing a straight chain of *n*-alkanes with a C_{15}-C_{18} range as the main compound [4]. In HDO, several reaction processes-namely decarboxylation (DCO_2), decarbonylation (DCO), and hydrogenation-may be involved [5,6].

So far, the use of natural zeolite (NZ) as a heterogeneous catalyst or as support material for generating hydrocarbon-based biofuel has rarely been explored. Several studies on green diesel production employing various heterogeneous catalysts have been conducted. Susanto *et al.* [7] reported the synthesis of renewable diesel from oleic acid as a model compound of triglyceride using a Pd/zeolite-Lampung (clinoptilolite [HEU] type) catalyst at a temperature of 375-400 °C and pressure of 15 bar H_2. The results showed 93.34% conversion of renewable diesel, with a selectivity and yield of the C_{13}-C_{19} fraction of 42.72% and 34.87%, respectively. Soni *et al.* [8] employed natural clay modified with a Ni/Co metal carrier metal as a catalyst for the conversion of methyl oleate/microalgae into green diesel. The result gave a total yield for the C_{12}-C_{22} alkane hydrocarbon chain of 84-86 wt.%. Solid state catalysts, such as zeolites, are a good choice to replace homogeneous catalysts, because they are able to serve two types of acidic sites at the same time. The acidic sites are Brønsted acid and Lewis acid sites which are useful during the catalytic process [9]. Moreover, the high chemical and physical stability levels of zeolite represent feasible features for application in high-pressure and temperature reaction conditions [10].

As a greener, inexpensive catalyst that is also highly selective, Fe was found to be partially oxidized by the carboxylic groups of the substrate during the reaction. Thus, the Fe-oxygen bonds that are formed can dictate the selectivity of the process to the successive conversion of carboxyl, first into carbonyl and then into alcohol intermediates [11]. In line with the study conducted by Zhou *et al.* [12] who used a mordenite [MOR]-type zeolite containing Fe in its skeleton, Fe exhibited excellent performance in catalytic reactions, especially in the DCO of dimethyl ether (DME), with the highest activity reaching 85% and decreased activity as the iron content increased. Iron catalytic species have also been used in the conversion of biomass-based feedstocks, such as: in transforming ethanol into liquid hydrocarbons on Zeolite Socony Mobil-5 [ZSM-5] [13]. The best conversion of liquid hydrocarbons was obtained with the samples with low iron content (0.3 wt.%), reaching a 30% yield.

Natural zeolite from Klaten Indonesia has been long studied for several purposes, such as: hydrocracking of LDPE plastic waste [14], pyrolysis and catalytic cracking [15,16], adsorption of heavy metal [17], and hydrocracking of waste lubricant oil [18]. Modification of these natural zeolites with several metals, i.e. Ni, Ni-Mo, Co, or Co-Mo [14,19], Ni-Pd [20], Zn [21], and Cu, Cr, or Pd [22], has also been conducted. However, the Fe modification and application of this material in catalyzing green diesel production has not been carried out. Therefore, the aim of this research is to study on the catalytic activity and selectivity of NZ and Fe modified NZ (Fe/NZ) in the production of green diesel from palm oil.

2. Materials and Methods

2.1 Materials

The NZ was obtained from Klaten, Central Java (particle size 170/240 mesh), $Fe(NO_3)_3 \cdot 9H_2O$ (Merck, 99.95%), refined palm oil (BIMOLI), aquadest (Bratachem, Indonesia), hydrogen and nitrogen (5.0 grade, ultra-high purity, were provided by SAMATOR Gas Indonesia).

2.2 Catalyst preparation

The Fe/NZ- was prepared using the wetness impregnation method. Impregnation was achieved by soaking the crushed NZ (4.85 g) in 60 mL of an aqueous solution containing 1.08 g $Fe(NO_3)_3 \cdot 9H_2O$ (3 wt.%) and stirred for 24 h. The mixture was then filtered and dried at room temperature for 24 h, and then it was continuously dried in an oven at 120 °C for 10 h. The resulting powder was calcined under nitrogen atmosphere for 2 h at 400 °C and followed by reduction under hydrogen flow for 2 h at 350 °C. The obtained material is then notifed as Fe/NZ.

2.3 Catalyst characterizations

The materials were characterized by powder X-ray diffraction (XRD), Fourier Transform

Infrared (FTIR), X-ray Fluorescence (XRF), Nitrogen adsorption-desorption, and Scanning Electron Microscopy-Energy dispersive X-ray spectroscopy (SEM-EDX). The XRD were recorded on a Philips X'pert MPD system using Cu-Kα radiation (X'Pert MPD diffractometer) with λ = 1.5406 Å and current held at 40 kV and 30 mA from the 2θ angle between 5 and 80°. Refinement was performed using the Le Bail method and RIETICA program. The XRF was measured on BRUKER S2 Ranger. The FTIR Shimadzu IR Prestige-21 was used by the method of KBr technique in the range 4000-400 cm^{-1}. The N_2 adsorption-desorption isotherms were measured in liquid N_2 at 77.3 K using an Autosorb-iQ (Quantachrome Co., USA). Total pore volume was estimated by measuring the volume of N_2 adsorbed at P/P_0 ~0.99. The specific surface areas were calculated using Brunauer-Emmett-Teller (BET) equation, while the pore size distribution was calculated from the desorption branch using the Barret-Joyner-Halenda (BJH) model. The SEM-EDX data were obtained from the Field Electron and Ion (FEI)-type Inspect S50.

2.4 HDO reaction of palm oil

Before the catalytic test, the reactor was sealed and purged with N_2 (30 minutes) to remove any oxygen content. The hydrogen gas was flowed with a pressure of 10 bar, and the temperature was slowly increased up to 375 °C for 2 h to ensure activity performance during the reaction. The palm oil was placed in a 100-mL batch-stirred autoclave reactor. A schematic representation of the experimental setup is shown in Figure 1. The refined palm oil (BIMOLI) was used as feed, and Fe/NZ was used as catalyst in comparison with NZ, with a feed ratio of 100:1 wt.% (oil:catalyst). The reactions were performed at a temperature of 375 °C with 12 bar of H_2 pressure for 2 h. The resulting gas was analyzed offline by using a Shimadzu GC-8A GC-thermal conductivity

Figure 1. Scheme of hydrodeoxygenation (HDO) reactor

detector (TCD) with a 6 m × 2 stainless steel packed adsorption column with a molecular sieve to identify CO_2, CO, and CH_4 released in every 15 minutes. The bottom product was distilled using a Koehler Model K 45090 with the American Society for Testing and Materials (ASTM)-D86 method. The HDO products were analyzed using Gas chromatography-mass spectroscopy (GC-MS) (Agilent Technologies 7890A gas chromatograph with an auto sampler and a 5975C mass selective detector) equipped with an HP-INNOWax capillary column (30 m × 0.25 mm × 0.20 μm film thickness). The measurements started at a 40 °C hold for 0.5 minute, rising at 8 °C/min to a 195 °C hold for 0 minute, and finally rising 1 °C/min to 225 °C and holding for 22 minutes. Helium was used as the carrier gas (1.8614 mL/minute), and an injection volume of 1 μL were used to identify the components in the HDO product.

2.5 Evaluation of HDO products

The conversion and selectivity of catalyst were defined according to Equations (1) and (2) refer to Liu *et al.* [23].

$$C = 100\% - C_{(TG)} \tag{1}$$

with $C_{(TG)}$ is the concentration of triglycerides (%) in the product oil determined by GC analysis. The selectivity of C_{15}-C_{18} hydrocarbon was calculated as:

$$S = Y_i/C \times 100\% \tag{2}$$

with Y_i is the yield of the C_{15}-C_{18} hydrocarbon (%), determined by GC analysis, and C is the conversion of palm oil (%) calculated by Equation (1).

3. Results and Discussion

3.1 Materials characterization

The main composition of NZ is SiO_2, while the others are Al_2O_3, Fe_2O_3, CaO, and K_2O as analyzed by XRF (Table 1a). It is well known that zeolite contains a structural unit [Si(OH)Al] that can act as Brønsted and Lewis acids, which is frequently used as a catalyst in a wide range of technological processes, such as petroleum refining and petrochemistry [24]. From Table 1a, the Si/Al ratio of NZ and Fe/NZ of about 4.72 and 5.83, respectively are in good agreement with an intermediate Si/Al ratio (Si/Al = 2-5) including MOR and HEU. These data also corresponds to the Brønsted acid sites
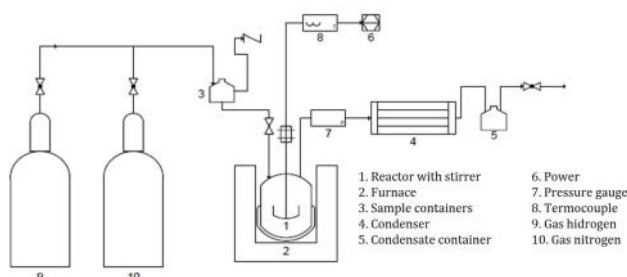
in the materials [25]. The lost number of aluminum atoms displaced from the network as increased Si/Al mol ratio of Fe/NZ. This behavior could be probably due to the substitution of Al^{3+} by Fe^{3+} in the tetrahedral position as observed in the previous report [26]. So, the increased of Si/Al mol ratio favors the raise in the amount of the acidity. According to XRF analysis (Table 1b) the iron content in NZ was found to be 3.03%, and increase in composition after Fe loading 3 wt.% in the Fe/NZ catalyst was about 6.04%. This value is in a line with the EDX analysis presented in Table 2. The presence of Fe on Fe/NZ is further confirmed by diffractogram at diffraction peak of $2\theta = 44$-$45°$ (JCPDS No. 06-0696) as shown in Figure 2. However, the peaks of Fe/NZ generally showed the same 2θ values as NZ and fit well with the MOR and HEU standard pattern. The presence of iron on the surface of NZ did not change the crystalline structure of the zeolite. It is well known that the positions and intensities of those peaks are essentially
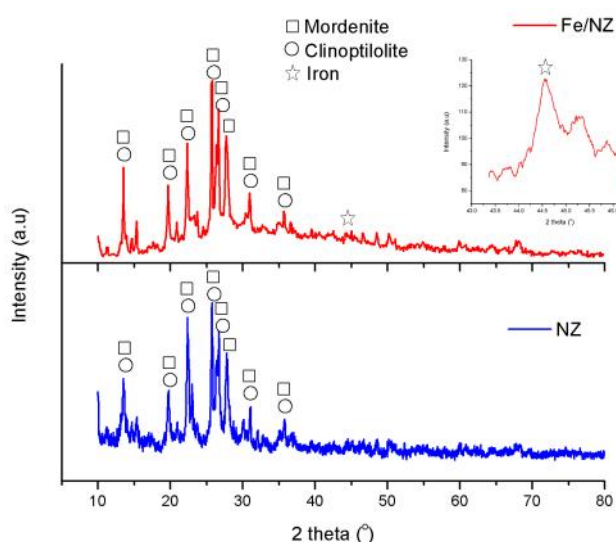
unchanged. The results indicated that NZ was stable and the Fe metal was not chemically incorporated into the zeolite framework. Small reflections of Fe^0 particles indicated that the small crystalline size of the iron and the crystallinity structure of the Fe [27].

Based on refinement process (shown in Figure 3), the refinement quality results in the XRD of Fe/NZ pattern with values of Residual phase (Rp) and Residual weight phase (Rwp) of 7.40 and 9.30, respectively. The refinement quality can be accepted by yielding values of Rp and Rwp less than 10. Smaller values indicate an increasingly perfect fit with the stan-

Table 2. Elemental composition of NZ and Fe/NZ determined by EDX

Element	NZ (wt.%)	Fe/NZ (wt.%)
Si	36.23	35.40
O	47.64	49.89
Al	8.95	7.58
Fe	1.07	4.47

Figure 2. Diffractogram of NZ and Fe/NZ
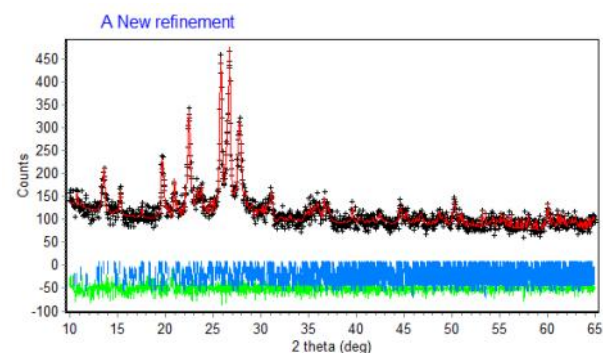
Figure 3. Observed (black), calculated (red) and difference (blue) curves of the refined Fe/NZ

Table 1. Metal-oxide (left) and elemental (right) composition of NZ and Fe/NZ determined by XRF

Element Formula	Concentration NZ (wt.%)	Concentration Fe/NZ (wt.%)
SiO_2	71.43	63.46
Al_2O_3	12.84	9.26
Fe_2O_3	4.34	8.64
CaO	5.53	5.33
K_2O	1.64	1.58
Si/Al mol ratio	4.72	5.83

Element Formula	Concentration NZ (wt.%)	Concentration Fe/NZ (wt.%)
Si	33.39	29.67
Al	6.79	4.90
Fe	3.03	6.04
Ca	3.95	3.81
K	1.36	1.31

dard phase. This shows that the Fe phase (JCPDS No. 06-0696) is identified and present in the Fe/NZ catalyst. The presence of the Fe phase is extremely important given that Fe(0) is an active species in the heterogeneous catalytic process [11].

Both NZ and Fe/NZ have an irregular spherical morphology that tends to be agglomerated and consist of an un-uniform particle size (Figure 4). However, Figure 4(b) shows that the 3 wt.% iron loading aggregated to form compact irregular shapes on the surface of the NZ support. This shows that the obtained NZ with Fe loading had formed fine clusters, indicating that the Fe species are well dispersed.

Based on FTIR spectra of the NZ (Figure 5), the range of 3440-3650 cm^{-1} wavenumbers indicated an OH stretching band from the silanol group. NZ and Fe/NZ showed a significant IR

peaks attributed to Si–O–Si bending (461 cm^{-1}), Si–O–Si symmetric stretching (796 cm^{-1}), Si–O–Si asymmetric stretching (1047cm^{-1}), and OH bending by silanol group (1639 cm^{-1}). FTIR spectra showed no major differences among the NZ and Fe/NZ frameworks, which indicated that impregnation of Fe does not affect the structure of the NZ. This result reinforces the discussion of previous XRD data in which the NZ framework remained intact after impregnation. Notably, the bands relating to NZ at 461, 796, 1047, and 1639 cm^{-1} were decreased by iron impregnation, which might be due to the formation of ferri-silicate groups (Si–O–Fe) in the framework as reported in previous works [28,29].

The total surface area was calculated based on the BET method via N_2 adsorption–desorption as shown in Figure 6(a). The materials exhibited type I adsorption isotherms typical of microporous solids with H4-type hysteresis loops, which are often associated with narrow slit-like pores indicative of microporosity [30]. The surface area, pore volume, and average pore size of NZ and Fe/NZ are summarized in Table 3. The BET surface area, pore volume, and average pore size inferred that impregnation of Fe on NZ has reduced the area. These effects may be attributed to the presence of Fe metal loading
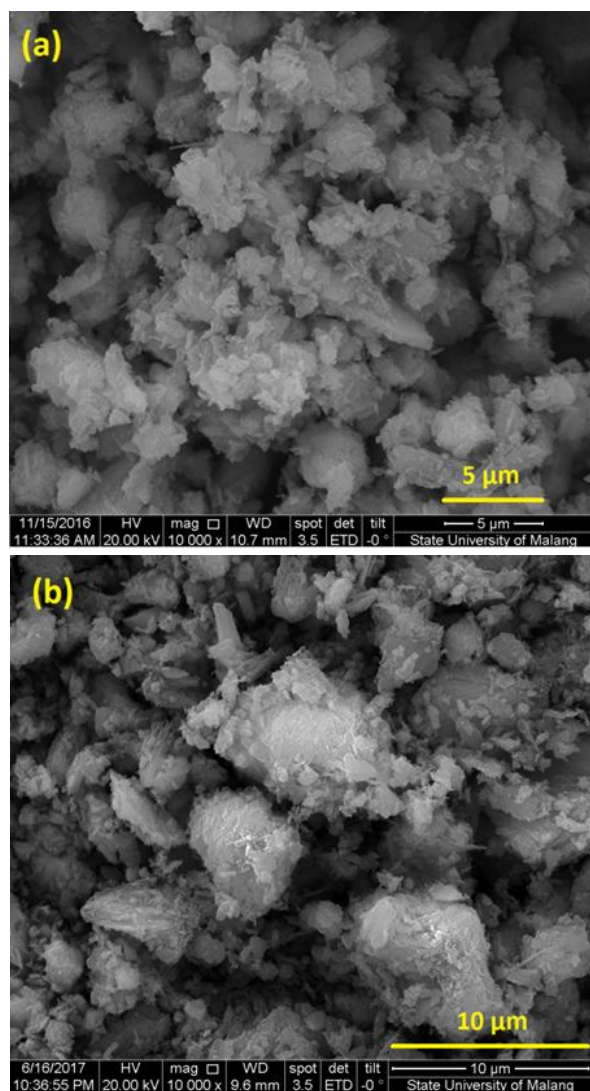

Figure 4. SEM images of NZ: (a) and Fe/NZ, (b) at a magnification of 10000X

Table 3. BET surface area and porosity of materials

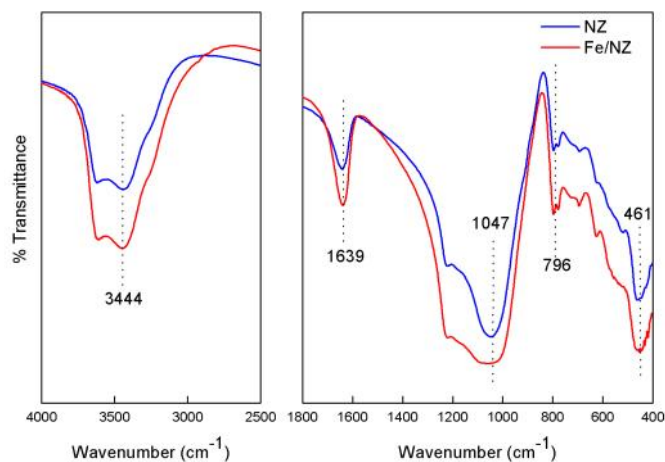| Materials	BET surface area (m^2/g)	Pore volume (cc/g)	Average pore size (Å)
NZ	55.41	0.09	33.38
Fe/NZ	51.26	0.07	26.49

Figure 5. FTIR spectra of NZ and Fe/NZ

favors micro-pore blocking [30]. NZ consists of crystalline microporous (<2 nm) alumino-silicate materials. The pore size distribution in Figure 6(b) shows that the parent NZ mainly contributed the microporosity. The micro-porous volume decreased, along with the average pore size of the Fe/NZ. The BET results and above XRD analysis indicate that the Fe could be impregnated inside the pores and/or on the external surface of the parent NZ, which is similar to the observations of Rostamizadeh *et al.* [31] over the modified ZSM-5.

3.2 Catalytic tests

The composition of vegetable oil plays an important role in the conversion factor for hydrotreating transformation into biohydrocarbons. The composition of vegetable oils to be processed by hydrotreating has a direct effect on the consumption of hydrogen, since unsaturated fatty acids will require higher hydrogen consumption during the hydrogenation process [4]. Table 4 shows the composition of palm oil used in this work in the form of triglycerides and contains unsaturated carboxylic acids with

Table 4. Fatty acid composition of refined palm oil (wt.% as methyl esters)

Fatty acid	Composition (wt.%)
$C_{16}:0$	38.13
$C_{18}:0$	3.08
$C_{18}:1$	41.85
$C_{18}:2$	11.43

oleic acid ($C_{18}:1$) composition of 41.85%, while palmitic acid ($C_{16}:0$) is only about 38.13% after hydrolysis treatment followed by methylation.

In general, the consumption of H_2 gas used to catalyzed palm oil decreased with time. This phenomenon is due to the added hydrogen gas consumed during the HDO reactions and auto-matically turned into several liquid and gas phases, such as: H_2O, CO, CO_2, CH_4, and propane, as already published in previous papers [32]. The rate of H_2 consumption obtained from this study using NZ and modification with Fe metal as heterogeneous catalysts can be seen in Figure 7. Based on the Figure 7, H_2 with an initial pressure of 12 bar on a Fe/NZ catalyst after 2 h reached a 100% v/v consumption level. This proved that the consumption rate of H_2 is influenced by the amount of metal present in the catalyst. In contrast to NZ, the H_2 consumption was about 80% v/v after a 2 h
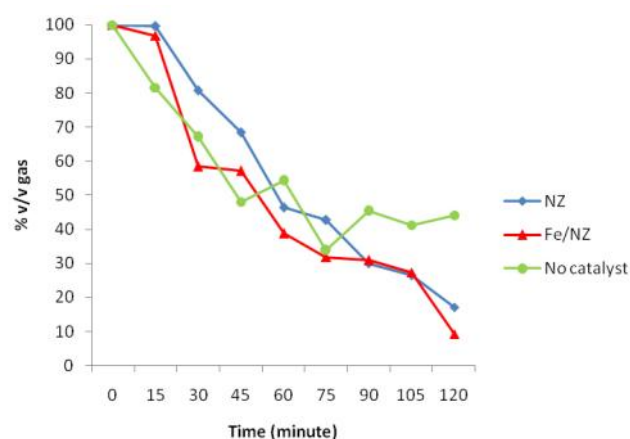

Figure 7. Rate of H_2 gas consumption at the initial pressure of 12 bar
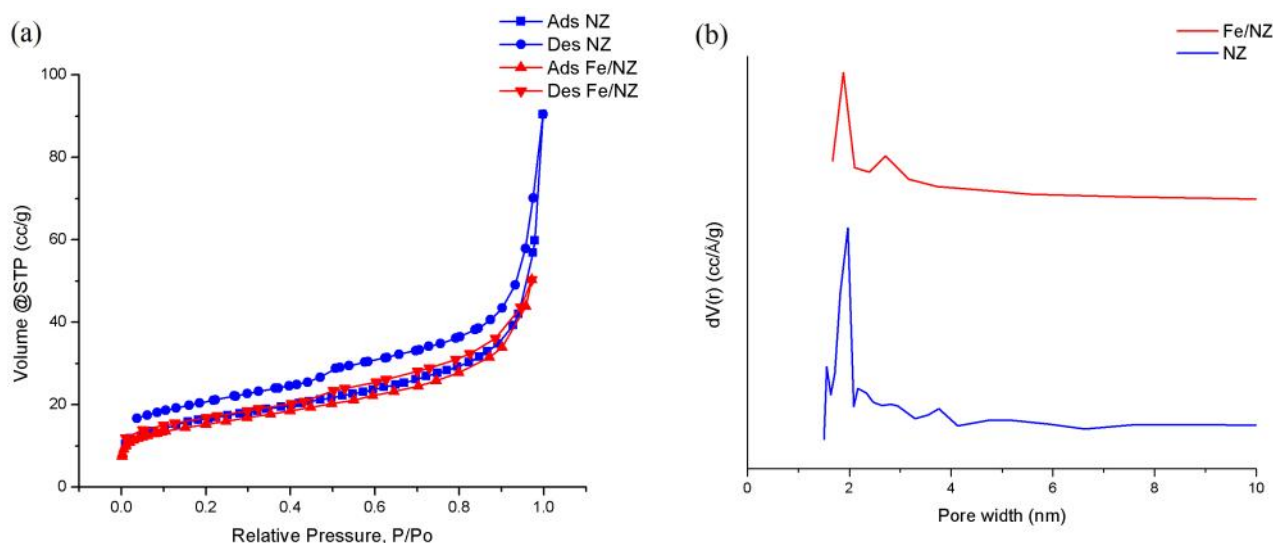

Figure 6. Nitrogen adsorption-desorption isotherm (a) and pore size distributions (b) of the materials

reaction, but this value is still higher than without the catalyst, where it reached more about 60% v/v. The rate of consumption without the catalyst for H_2 gas was relatively lower than that of NZ and Fe/NZ. Huang *et al.* [33] suggested that iron-based catalyst can improve the hydrogen transfer. Therefore, the addition of iron-based catalyst increased the yield of bio-oil. It can be concluded that the catalyst can speed up the chemical reaction and provide an alternative route for the reaction.

The effectiveness of NZ and Fe/NZ in the deoxygenation and saturation of the C=C double bond to produce *n*-paraffin products in the range of boiling points of diesel oil can be determined based on the product gas during the catalytic process. Based on the analysis of gas formation rate curve using GC-TCD analysis on the NZ and Fe/NZ catalysts (Figure 8), it was possible to determine the type of reaction that took place during the catalytic process, which could be HDO, cracking, or isomerization.

The DCO and DCO_2 reaction broke the oxygen bond, so that the alkane bond could be produced, indicating that the levels of CO and CO_2 gas were moderate, at approximately 20% on NZ started 0 minutes after reaction temperatures have reached at 375 °C and 12 bar H_2. However, the production of CO and CO_2 for Fe/NZ showed below the detection limit (LOD) GC-TCD cause the extrapolated data of gas product. As discussed in GC-MS analysis, the product has a higher composition in diesel fraction but showed the low amount of CO and CO_2 gas. It could be due to the difficulty in desorption of gas product from the Fe/NZ surface at high reaction pressure. Thus, the desorption CO and CO_2 gas of NZ was inhibited the occurrence of internal mass transfer due to the presence of high amount Fe in the surface observed by XRF and EDX analysis. Furthermore, slight increases in the formation of CO and CO_2 was

observed without catalyst may be due to the most abundant gas component was unreacted hydrogen suggested produced the insignificant (reverse) water-gas shift reaction ($H_2 + CO_2 \leftrightarrow CO + H_2O$) as reported previously by Zhao *et al.* [34] who produced high content of CO and CO_2 gas over ZSM-5 catalyst. However, the production of CO and CO_2 without catalyst for this experimental conditions showed below the detection limit (LOD) caused the low content obtained (data not shown). The competitive adsorption of H_2 and palm oil molecules on the catalyst surface needs detailed kinetic study to verify. The production of methane could also be detected with GC-TCD, but the content was still in relatively low below the detection limit of less than 0.2% (the data are not shown here). This result shows that both catalysts can minimize the production of methane so that the alkene bond, which is an undesirable product called a cracking product, was not formed.

The liquid product analysis showed that the main distillation product of the diesel hydrocarbon fraction generally consisted of a straight chain of *n*-alkanes (C_{15}-C_{18}). Figure 9
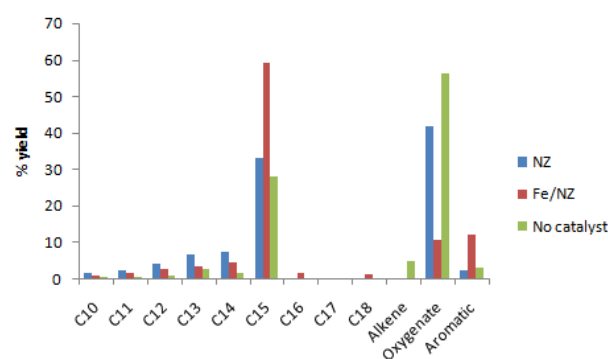
Figure 9. Liquid yield product distribution of NZ, Fe/NZ, and no catalyst in the hydrodeoxygenation reaction of refined palm oil at 375 °C, 12 bar H_2, and 2 h
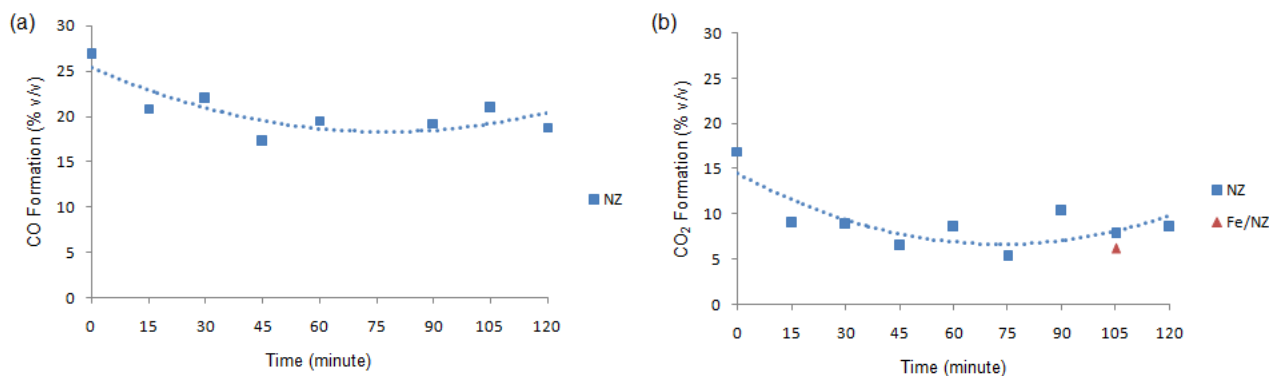
Figure 8. Gas rate formation curve: (a) carbon monoxide, and (b) carbon dioxide

shows the yield of *n*-paraffins in the HDO reaction of palm oil with the NZ and Fe/NZ catalysts. The palm oil was converted to green diesel products that mostly contained *n*-paraffin C_{10}-C_{18} hydrocarbons (Table 5).

From Table 5, it can also be seen that the largest conversion of reactants occurred in the Fe/NZ is 89.18%, while the result for NZ is about 58.32%. Comparably to the conversion, Fe/NZ also had the largest selectivity on the C_{15}-C_{18} fraction (diesel fraction), with 66.37% and 1.55% of selectivity for C_{15} and C_{18}, respectively. The Fe/NZ also produced the smallest percentage of oxygenated fraction compared to NZ and without a catalyst, as this contained fatty acid or methyl esters. In addition, both material catalysts still generated some product contents, such as: aromatics, carboxylates, and alkenes. This result suggests that palm oil is not fully converted to diesel-range hydrocarbons. However, the work still demonstrated not only high efficiency but also selectivity for deoxygenation reactions from palm oil to biohydrocarbons of the diesel range C_{15}-C_{18}. Based on Figure 9 and Table 5, it can be stated that the most abundant composition in liquid hydrocarbon products was *n*-pentadecane (C_{15}), with higher selectivity on Fe/NZ than on NZ or no catalyst. It can be assumed that the C_{15} products generated through the DCO/DCO$_2$ route during the hydroconversion of palm oil were the same as those indicated by Deliy *et al*. [35] and Xin *et*

Table 5. Liquid product distribution of HDO reaction

Compound	NZ (%)	Fe/NZ (%)	No Catalyst (%)
C_{10}	1.78	0.93	0.85
C_{11}	2.38	1.84	0.85
C_{12}	4.47	3.04	1.03
C_{13}	6.78	3.44	3.01
C_{14}	7.48	4.67	1.63
C_{15}	33.04	59.19	28.32
C_{16}	0	1.8	0
C_{17}	0	0	0
C_{18}	0	1.39	0
Alkene	0	0.47	4.97
Oxygenate	41.68	10.82	56.18
Aromatic	2.39	12.41	3.16
% Green diesel	55.93	76.3	35.69
% Conversion	58.32	89.18	43.82
% Selectivity C_{15}	56.65	66.37	64.62
% Selectivity C_{16}	0	2.01	0
% Selectivity C_{17}	0	0	0
% Selectivity C_{18}	0	1.55	0
% Total product	100	100	100

al. [36] who used a Ni-based catalyst in converted methyl palmitate into green diesel.

Our observations of NZ and no catalyst process indicated that no chains of C_{16}, C_{17}, and C_{18} were established during the hydroconversion process compared to the Fe/NZ catalyst. This shows the lack of selectivity of the NZ and no catalyst process in producing C_{17} chains by the reaction of DCO/DCO$_2$ and C_{16} or C_{18} chains produced by the HDO reaction. This indicates that the NZ contains a low acidity compared to the Fe/NZ catalyst. This phenomenon is inline with the acidity data reflected from Si/Al mol ratio which has been previously discussed. The addition of metals to a zeolite support promises to be useful in generating heterogeneous catalysts, as they can act as Lewis acid sites. Lewis acid sites play a key role in the activity and selectivity of catalysts against liquid product yields [37] as reported by Deng *et al*. [27] indicating the presence of new Lewis acids sites on the Fe sites of Fe/Beta catalysts. Hong *et al*. [38] also found that Fe based catalysts are promising for hydro-deoxygenation (HDO) due to their high selectivity a direct C–O bond cleavage.

The proposed reaction mechanism in HDO palm oil can be seen in Figure 10. Mechanisms that may be occurred are likely to include three pathways by which oxygen can be removed from the triglycerides, as follows: hydrogenation, DCO$_2$, and DCO. The triglycerides are first hydrogenated to saturated ones at around 200 °C [39] and then convert to intermediates, such as monoglycerides, diglycerides, ketones, aldehydes, and carboxylic acids. These are formed in the initial step and subsequently hydrogenated or broken down via DCO$_2$, DCO, or HDO. Based on GC-MS analysis, the liquid products produced in this work tend to selectively produce the C_{15}-C_{18} diesel range. This indicates that the iron catalyst used in this work remained to be highly active, selective, and favorable for contributing in the conversion of palm oil to the diesel fraction.

Based on the FTIR analysis in Figure 11, it can be seen that the characteristic peak of the C=O stretch in triglyceride esters that are predominantly found in wavenumber of 1711 cm^{-1}, which is a characteristic strain of carboxylic acid [4]. These intensities shows that the HDO process produced a high level of efficiency indicated by the reducing the intensity or transmittance (%T) of C=O peaks in refined palm oil. The decreased transmittance ratio of spectra (C=O/C–H) reflects the decreased oxygen content of the products. In this case, the transmittance ratio of C=O/C–H in palm oil

was about 0.98 decreased to 0.5, 0.77, and 0.94 when Fe/NZ, NZ, and no catalyst process, respectively, were used. This results support well the proposed mechanism as discussed previously (Figure 10). The FTIR spectrum of the green diesel also showed characteristic vibration bands of saturated hydrocarbon (C–H) stretching within the region of 2850-3000 cm^{-1} or the band at 1350-1480 cm^{-1} relating to the bending of C–H methyl groups [40].
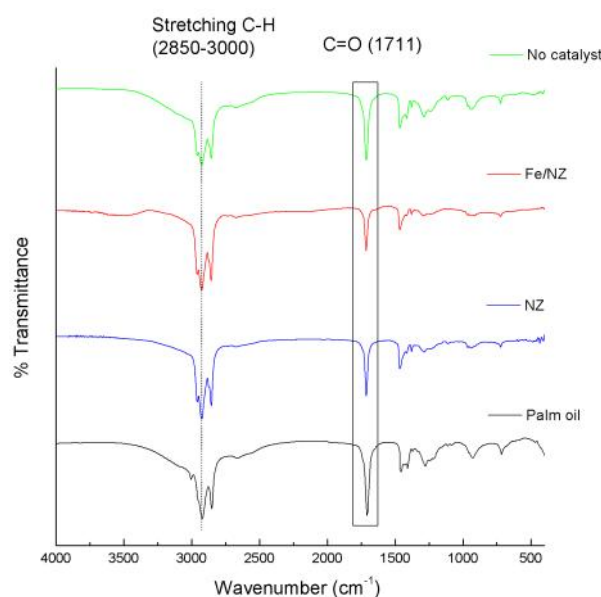
4. Conclusions

NZ shows crystallinity and suitability with the simulated pattern of MOR and HEU phases. The presence of Fe metal on the surface and pore of NZ had no significant influence on the crystal structure and morphology, but it did have a significant effect on catalytic activity and selectivity. The most abundant products from the HDO reaction in this work was a liquid hydrocarbon with straight chain (C_{15}-C_{18}) alkanes. The liquid yield product exhibited a higher conversion into diesel-like hydrocarbons, reaching more than 58% and 89% when the NZ and Fe metal loading (3 wt.%) catalysts, respectively, were used. Further research on the effect of dealumination of NZ and percent variation of Fe metal addition into activated and nonactivated NZ as a catalyst in green diesel production is also currently being done in our group.

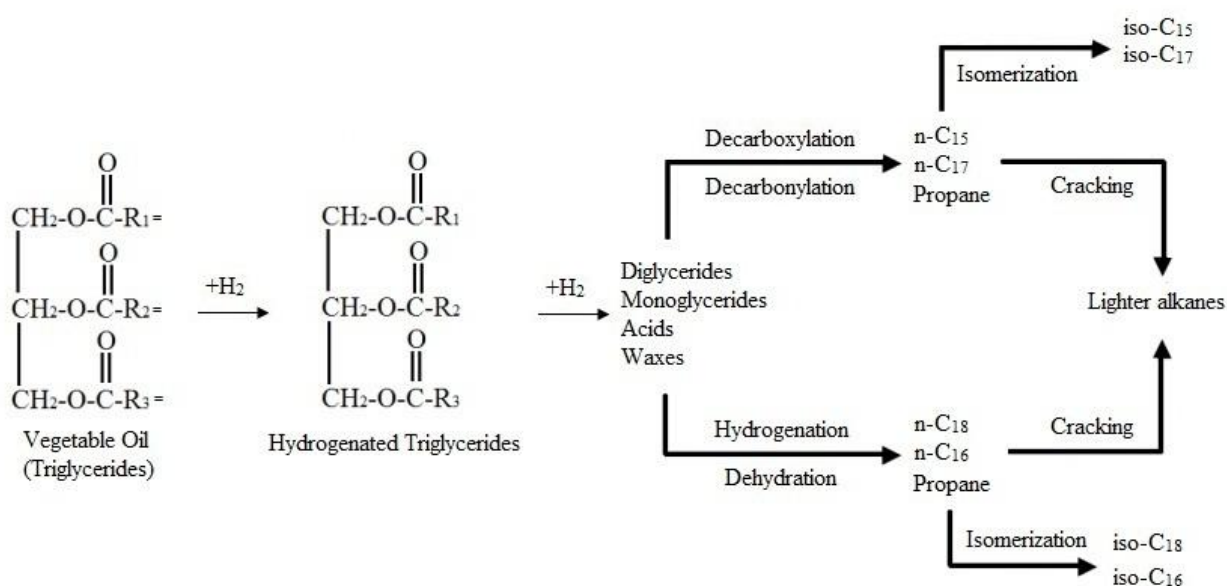**Figure 11**. FTIR spectra of the HDO products

Figure 10. Possible mechanism of hydrodeoxygenation (HDO) of triglycerides to alkanes refer to Huber *et al*. [41] with modifications

References

[1] Orozco, L.M., Echeverri, D.A., Sánchez, L., Rios, L.A. (2017). Second-generation Green Diesel from Castor Oil: Development of a New and Efficient Continuous-production Process. *Chem. Eng. J.*, 322: 149-156.

[2] Kusuma, R.I., Hadinoto, J.P., Ayucitra, A., Soetaredjo, F.E. (2013). Natural Zeolite from Pacitan Indonesia, as Catalyst Support for Transesterification of Palm Oil. *Appl. Clay Sci.*, 74: 121-126.

[3] Wang, Q., Gupta, N., Wen, G., Bee, S. (2017). Palladium and Carbon Synergistically Catalyzed Room-temperature Hydrodeoxygenation (HDO) of Vanillyl Alcohol-A Typical Lignin Model Molecule. *J. Energy Chem.*, 26: 8-16.

[4] de Sousa, F.P., Cardoso, C.C., Pasa, V.M.D. (2016). Producing Hydrocarbons for Green Diesel and Jet Fuel Formulation from Palm Kernel Fat over Pd/C. *Fuel Process. Technol.*, 143: 35-42.

[5] Veriansyah, B., Han, J.Y., Kim, S.K., Hong, S.A. (2012). Production of Renewable Diesel by Hydroprocessing of Soybean Oil: Effect of Catalysts. *Fuel* 94: 578-585.

[6] Kaewmeesri, R., Srifa, A., Itthibenchapong, V., Faungnawakij, K. (2015). Deoxygenation of Waste Chicken Fats to Green Diesel over Ni/Al$_2$O$_3$: Effect of Water and Free Fatty Acid Content. *Energ. Fuel.* 29: 833-840.

[7] Susanto, B.H., Nasikin, M., Wiyo, A. (2014). Synthesis of Renewable Diesel through Hydrodeoxygenation Using Pd/Zeolite Catalysts. *Procedia Chem.*, 9: 139-150.

[8] Soni, V.K., Sharma, P.R., Choudhary, G., Pandey, S., Sharma, R.K. (2017). Ni/Co-Natural Clay as Green Catalysts for Microalgae Oil to Diesel-Grade Hydrocarbons Conversion. *ACS Sustain. Chem. Eng.*, 5(6): 5351-5359.

[9] Wang, Z., Wang, L., Jiang, Y., Hunger, M. (2014). Cooperativity of Brønsted and Lewis Acid Sites on Zeolite for Glycerol Dehydration. *ACS Catal.*, 4: 1144-1147.

[10] Cubillas, P., Anderson, M.W., Strohmaier, K.G., Wright, P.A. (2011). Zeolites and Catalysis. *Reactions*, 50: 5425-5426.

[11] Kandel, K., Anderegg, J.W., Nelson, N.C., Chaudhary, U. (2014). Supported Iron Nanoparticles for the Hydrodeoxygenation of Microalgal Oil to Green Diesel. *J. Catal.*, 314: 142-148.

[12] Zhou, H., Zhu, W., Shi, L., Liu, H. (2015). Promotion Effect of Fe in Mordenite Zeolite on Carbonylation of Dimethyl Ether to Methyl Acetate. *Catal. Sci. Technol.*, 5: 1961-1968.

[13] Calsavara, V., Luciano, M. (2008). Transformation of Ethanol into Hydrocarbons on ZSM-5 Zeolites Modified with Iron in Different Ways. *Fuel*. 87: 1628-1636.

[14] Sriningsih, W., Saerodji, M.G., Trisunaryanti, W., Armunanto, R. (2014). Fuel Production from LDPE Plastic Waste over Natural Zeolite Supported Ni, Ni-Mo, Co, and Co-Mo Metals. *Procedia Environ. Sci.*, 20: 215-224.

[15] Nasser, G.A., Kurniawan, T., Tago, T, Bakare, I.A. (2015). Cracking of n-hexane over hierarchical MOR zeolites derived from natural minerals. *J. Taiwan Inst. Chem. Eng.* 61: 20-25.

[16] Syamsiro, M., Saptoadi, H., Norsujianto, T., Noviasri, P. (2014). Fuel oil production from municipal plastic wastes in sequential pyrolysis and catalytic reforming reactors. *Energy Procedia* 47: 180-188.

[17] Mudasir, M., Karelius, K., Aprilita, N.H., Wahyuni, E.T. (2016). Adsorption of mercury(II) on dithizone-immobilized natural zeolite. *J. Environ. Chem. Eng.* 4: 18391849.

[18] Trisunaryanti, W., Syoufian, A., Purwono, S. (2013). Characterization and Modification of Indonesian Natural Zeolite for Hydrocracking of Waste Lubricant Oil into Liquid Fuel Fraction. *J. Chem. Chem. Eng.* 7: 175-180.

[19] Trisunaryanti, W., Triwahyuni, E., Sudiono, S. (2005). Preparasi, Modifikasi dan Karakterisasi Katalis Ni-Mo/zeolit alam dan Mo-Ni/Zeolit alam. *Teknoin*, 10: 269-282.

[20] Trisunaryanti, W., Triwahyuni, E., Sudiono, S. (2005). Preparation, Characterizations and Modification of Ni-Pd/Natural Zeolite Catalysts. *Indo. J. Chem.* 5: 48-53.

[21] Trisunaryanti, W., Purwono, S., Putranto, A. (2008). Catalytic Hydrocracking of Waste Lubricant Oil into Liquid Fuel Fraction using ZnO, Nb$_2$O$_5$, Activated Natural Zeolite, and Their Modification. *Indonesian Journal of Chemistry* 8: 342-347.

[22] Trisunaryanti, W, Rizki, C.N., Saptoadi, H., Syamsiro, M. (2013). Characteristics of Metal Supported-Zeolite Catalysts for Hydrocracking of Polyethylene Terephthalat. *IOSR J. Appl. Chem.* 3: 29-34.

[23] Liu, J., He, J., Wang, L., Li, R. (2016). NiO-PTA Supported on ZIF-8 as a Highly Effective Catalyst for Hydrocracking of Jatropha Oil. *Sci. Rep.* 6: 23667.

[24] Arean, C.O., Nachtigall, P., Thang, V., Bula, R. (2014). Measuring the Brønsted Acid Strength of Zeolites-Does It Correlate with the O–H Frequency Shift Probed by a Weak Base? *Phys. Chem. Chem. Phys.* 16: 10129-10141.

[25] Sommer, J., Louis, B. (2004). Quantitative Determination of Brønsted Acid Sites on Zeolites: A New Approach towards the Chemical Composition of Zeolites. *Catal. Letters*. 93: 81-82.

[26] Ko, Y.S., Jang, H.T., Ahn, W.S. (2008). Hydrothermal synthesis and characterization of Fe(III)-substituted mordenites. *Korean J. Chem. Eng.* 25: 1286-1291.

[27] Deng, J., Liu, J., Song, W., Zhao, Z. (2017). Selective Catalytic Reduction of NO with NH_3 over Mo-Fe/Beta Catalysts: The Effect of Mo Loading Amounts. *RSC Adv.* 7: 7130-7139.

[28] Sazegar, M.R., Dadvand, A., Mahmoudi, A. (2017). Novel Protonated Fe-containing Mesoporous Silica Nanoparticle Catalyst: excellent performance cyclohexane oxidation. *RSC Adv.* 7: 27506-27514.

[29] Mat, R., Amin, N.A.S. (2015). Fe/HY Zeolite as an Effective Catalyst for Levulinic Acid Production from Glucose: Characterization and Catalytic Performance. *Appl. Catal. B Environ.* 163: 487-498.

[30] Kragović, M., Daković, A., Marković, M., Krstić, J. (2013). Characterization of Lead Sorption by the Natural and Fe(III)-modified Zeolite. *Appl. Surf. Sci.* 283: 764-774.

[31] Rostamizadeh, M, Yaripour, F. (2016). Bifunctional and bimetallic Fe/ZSM-5 nanocatalysts for methanol to olefin reaction. *Fuel* 181: 537-546.

[32] Zhou, L., Lawal, A. (2016). Hydrodeoxygenation of Microalgae Oil to Green Diesel over Pt, Rh and Presulfided NiMo Catalysts. *Catal. Sci. Technol.* 6: 1442-1454.

[33] Huang, H.J., Yuan, X.Z., Zeng, G.M., Liu, Y. (2013). Thermochemical liquefaction of rice husk for bio-oil production with sub-and supercritical ethanol as solvent. *J. Anal. Appl. Pyrolysis*. 102: 60-67.

[34] Zhao, X., Wei, L., Cheng, S., Huang, Y. (2015). Catalytic cracking of camelina oil for hydrocarbon biofuel over ZSM-5-Zn catalyst. *Fuel Process. Technol.* 139: 117-126.

[35] Deliy, I.V., Vlasova, E.N., Nuzhdin, A.L., Gerasimov, E.Y. (2014). Hydrodeoxygenation of Methyl Palmitate over Sulfided Mo/Al_2O_3, $CoMo/Al_2O_3$ and $NiMo/Al_2O_3$ Catalysts. *RSC Adv.* 4: 2242-2250.

[36] Xin, H., Guo, K., Li, D., Yang, H. (2016). Production of high-grade diesel from palmitic acid over activated carbon-supported nickel phosphide catalysts. *Appl. Catal. B Environ.* 187: 375-385.

[37] Zhao, X., Wei, L., Cheng, S., Julson, J. (2017). Review of Heterogeneous Catalysts for Catalytically Upgrading Vegetable Oils into Hydrocarbon Biofuels. *Catalysts*. 7: 83.

[38] Hong, Y., Wang, Y. (2017). Elucidation of reaction mechanism for m-cresol hydrodeoxygenation over Fe based catalysts: A kinetic study. *Catal. Commun.* 100: 43-47.

[39] Duan, J., Han, J., Sun, H., Chen, P. (2012). Diesel-like Hydrocarbons Obtained by Direct Hydrodeoxygenation of Sunflower Oil over Pd/Al-SBA-15 Catalysts. *Catal. Commun.* 17: 76-80.

[40] da Mota, S.D.P., Mancio, A.A., Lhamas, D.E.L., de Abreu, D.H. (2014). Production of Green Diesel by Thermal Catalytic Cracking of Crude Palm oil (*Elaeis guineensis Jacq*) in a Pilot Plant. *J. Anal. Appl. Pyrolysis*. 110: 1-11.

[41] Huber, G.W., O'Connor, P., Corma, A. (2007). Processing Biomass in Conventional Oil Refineries: Production of High Quality Diesel by Hydrotreating Vegetable Oils in Heavy Vacuum Oil Mixtures. *Appl. Catal. A Gen.* 329: 120-129.